Appl Phys B (2010) 100: 591–595
DOI 10.1007/s00340-010-4117-4

Applied Physics B
Lasers and Optics

Fast and stable enhancement of the far-field peak power by use of an intracavity deformable mirror

P. Yang · X. Lei · R. Yang · M. Ao · L. Dong · B. Xu

Received: 21 July 2009 / Revised version: 5 June 2010 / Published online: 10 July 2010

Abstract We demonstrate that an intracavity deformable mirror (DM) is capable of compensating for the aberrations of a continuous-wave (CW) Nd:YAG solid-state laser and improving its far-field peak power fast and stably. The deformable mirror is controlled by a stochastic parallel gradient descend (SPGD) algorithm. Experimental results reveal that high-order-like transverse modes can be transformed into Gaussian-like modes quickly without any pinhole added in the laser cavity. At the same time, the far-field peak powers are also increased to different extents.

1 Introduction

It is known that when a solid-state laser operates in a multi-transverse mode oscillation, the output beam quality is usually too poor to satisfy many applications [1–5]. In contrast to the multimode operation status, the fundamental transverse mode operation has smaller beam divergence and higher beam quality. Thus, making a solid-state laser producing a relatively high-power and high beam quality output is one of the most promising research orientations for more and more solid-state laser researchers. Generally, for obtaining a high beam quality, a simple way one may think is to introduce a pinhole into the laser resonator to restrict high-order transverse modes for selecting out the fundamental mode. However, choosing this way is not wise since it will inevitably result in a significant debasing of the output power. In most cases, the thermal effects in solid-state laser resonators are the main distortions to deteriorate the output laser beam quality. Therefore, they have to be corrected for obtaining high beam quality. Many ways (such as designing an appropriate cavity configuration or choosing an excellent laser rod and so on) have been employed to remove thermal effects [4]; unfortunately, though these ways and means may overcome static thermal effects partly, they are incapable of eliminating dynamic thermal distortions completely. Since thermal distortions in the resonators change with the pumping conditions [6], thereby the promising ways for compensating the thermally induced aberrations are to employ adaptive methods. It is known that adaptive optics (AO) technique is a powerful technique that allows for dynamic correction of phase aberrations [7]. Although it is initially developed for compensating for the turbulence of atmosphere, it has also been using for beam cleanup in many laser fields [8–14]. Deformable mirrors (DM) have been taken as the intracavity rear mirrors of solid-state laser resonators to optimize the output transverse modes [13, 14]. However, in one way, it often takes a long time to obtain good results, in another way, the published papers are often just concerning the conversion of the lower transverse modes into fundamental mode without describing the enhancement of peak power in the far-field. To overcome these disadvantages mentioned above, in this paper, we present a fast and stable adaptive solid-state resonator for correcting intracavity aberrations and enhancing the far-field peak power. A SPGD algorithm is employed as the control

P. Yang (✉) · X. Lei · L. Dong · B. Xu
The Key Laboratory on Adaptive Optics, Chinese Academy of Sciences, Chengdu 610209, China
e-mail: pingyang2516@163.com
Fax: +86-28-85100433

P. Yang · X. Lei · L. Dong · B. Xu
Institute of Optics and Electronics, Chinese Academy of Sciences, Shuangliu, Chengdu 610209, China

R. Yang · M. Ao
School of Optoelectronic Information, University of Electronic Science and Technology of China, Chengdu 610054, China

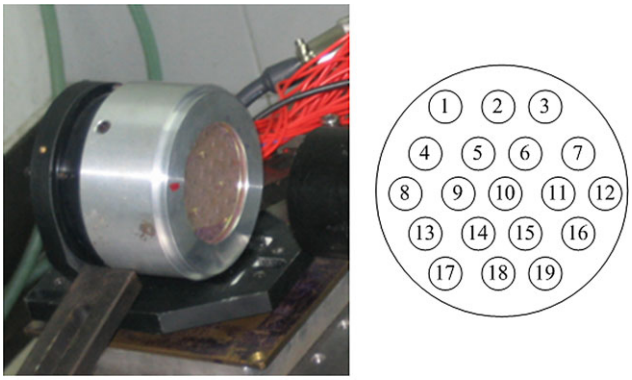

Fig. 1 The DM fabricated in our lab. (**a**) Photograph of the DM, (**b**) the actuator distributions of the 19-element DM of which each numbered circle represents an actuator

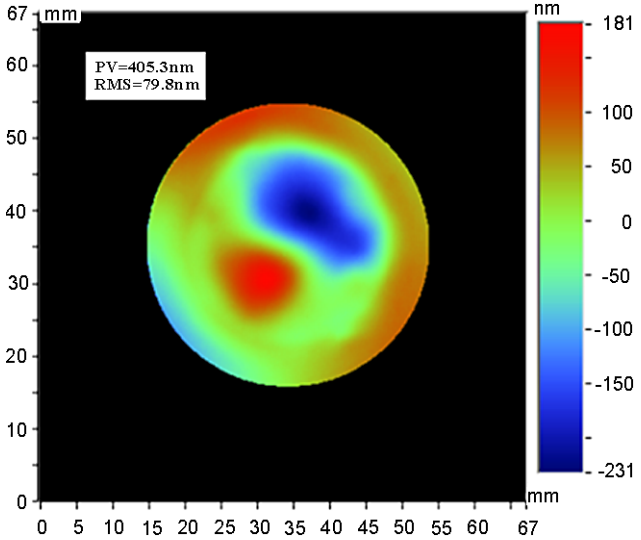

Fig. 2 The original surface DM shape measured by a WYKO interferometer

method for controlling the DM to correct aberrations and improve the far-field peak power. This paper is arranged as the follows: we will firstly introduce the basic theory of 19-element DM which is taken as the intracavity rear mirror in Sect. 2, and then describe the principle of SPGD algorithm and its actual application in Sect. 3; at last, the experimental results at different initial states are given in Sect. 4.

2 The 19-element intracavity DM

A schematic of the mirror actuators distributions, together with photograph of the mirror, is shown in Fig. 1. The 19-element DM is fabricated in our lab and has a continuous face plate with stacked PZT actuators [15], the parameters are as follows: effective area 32×32 mm^2, maximum deflection ± 2 μm, maximum voltage ± 300 V, resonance frequency > 10 kHz, thermal damage threshold value > 3 kW/cm^2 . According to its principle, the DM deforms its surface when applying voltages on the actuators:

$$\varphi(x, y) = \sum_{j=1}^{n} v_j V_j(x, y) \tag{1}$$

where $\phi(x, y)$ relates to the mirror shape, v_j is the voltage applied onto the jth actuator, $V_j(x, y)$ is the influence function of the jth actuator on the wavefront, n is the serial number of actuators.

The influence function of the DM can be expressed as

$$V_j(x, y) = \exp\left[\ln(w)\left(\sqrt{(x - x_j)^2 + (y - y_j)^2}/d\right)\right]^2 \tag{2}$$

where w is the coupling coefficients of DM. It is more convenient for this DM to fit some surface shapes when the value of w is large; however, the larger the w, the stronger one actuator's influence on its neighboring actuators, which will affect the correction precision. Therefore, this value should be chosen properly when designing DM, and more often than not it is in the range of 5% to 15%. As a result, w is set to 10% in this paper; (x_j, y_j) is the space position of the jth actuator, d is the distance between every two neighboring actuators and set at 8 mm, x and y represent the value in x-coordinate and y-coordinate of the orthogonal coordinate plane.

Figure 2 is the original DM surface shape measured by a WYKO interferometer whose specifications are as follows: peak-to-valley (PV): $\pm 1/20$ μm, root-mean-square (RMS) $\pm 1/120$ μm. The measured results show that the PV and RMS of the original DM surface are about 405.3 nm and 79.8 nm respectively, which means that the quality of the original DM surface is adequate.

3 SPGD algorithm and its application in this system

For the conventional AO systems used in astronomy, the aberrated wavefront must be first determined before the application of its conjugate; therefore, wavefront-sensors are often indispensable in these systems.

Nevertheless, when an AO system is employed, with intracavity to enhance the output beam performance of CW solid-state lasers, it is difficult or even impossible to measure the wavefront aberration and apply a conjugation correction for achieving promising outcomes just through the same way. The main reason lies in the fact that a CW AO laser system is a regenerative system: any DM shape change will modify intracavity laser modes. Therefore, the thermal distribution within the gain medium is changed, and as such, so does the search field. This will prevent the use of a typical astronomical AO system in CW laser systems. Besides,

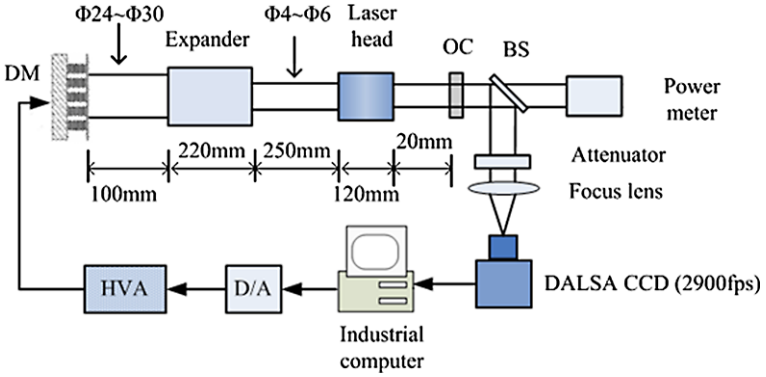

Fig. 3 The schematic configuration of intracavity AO system based on SPGD

there is still no precise mathematical model of the relation between the intracavity aberrations and the output beam quality, therefore, the measured ex-cavity beam quality cannot represent the intracavity aberrations with a linear relationship. Therefore, it is impossible to ascertain the actual aberrations in the resonator just though ex-cavity wavefront measurement. Compared with a conventional AO technique, a new AO scheme based on an SPGD algorithm which does not have to measure the phase aberrations can solve the problem. It is adopted to control the intracavity DM to compensate for phase aberrations of the solid–state laser and enhance its far-field peak power in this paper.

The theory of SPGD algorithm is described in detail in [16]; as for the SPGD algorithm employed in our system, the power-in-a-bucket (PIB) of far-field (the total intensity within 7×7 pixels of the CCD camera is taken as the PIB) is taken as the cost function $J^{(k)} = J(u^k_{1,}, u^k_{2,}, \ldots, u^k_{19,})$, where $u^k_{1,}, u^k_{2,}, \ldots, u^k_{19,}$ are the voltages applied onto the 19 actuators of the DM during the kth iterative calculation. The SPGD algorithm is a fast iterative algorithm whose iteration cycle is as follows.

(1) Generate a group of statistically independent random small amplitude perturbation voltages $\delta u^k_{1,}, \delta u^k_{2,}, \ldots, \delta u^k_{19}$.
(2) Apply the "positive" perturbation array $(u^k_1 + \delta u^k_{1,}, u^k_2 + \delta u^k_2, \ldots, u^k_{19} + \delta u^k_{19})$ onto the 19 actuators of the DM, and then calculate the PIB J^k_+.
(3) Similarly, apply the "negative" random perturbation array $(u^k_1 - \delta u^k_{1,}, u^k_2 - \delta u^k_2, \ldots, u^k_{19} - \delta u^k_{19})$ onto the 19 actuators, then calculate another PIB: J^k_-.
(4) Update the voltages according to: $u^{k+1}_i = u^k_i + \gamma \delta u^k_i \times (J^k_+ - J^k_-)$ $i = 1, 2, \ldots 19$, where γ is the gain coefficient, and δ is the metric perturbation. The value of γ and δ will determine the convergence rate and the actual performance. Generally, the larger the γ and δ, the larger the gap between the actual performance and optimal performance, from this point of view, γ and δ should be small. However, the convergence rate is proportional with γ and δ; therefore, when γ and δ are small, the convergence rate will become slow. Thus we should make a compromise for choosing a moderate γ and δ, and as a result, they are set to 0.003 and 0.04 respectively.

The schematic experiment configuration is shown in Fig. 3. The laser rod used is a lamp-pumped Nd:YAG rod which has a diameter of 6.5 mm and a length of 120 mm, the max pumping power is about 1000 W and can maximally generate 40 W output when operated in a multimode resonator. Generally, a conventional solid-state laser is composed of a rear mirror, a laser head and an output coupler (OC). However, in our system, there is an obvious difference from the conventional ones: the 19-element DM is used as the intracavity rear mirror. The intracavity beam aperture (about $\varnothing 4 \sim 6$ mm) changes with the pumping power, a $6\times$ telescope is used as the expander to make the beam cover at least 70% of the DM aperture. The distances between the optical elements in the resonators are labeled in Fig. 3.

The output beam is then divided into two parts by a beam splitter (BS). The transmitting part is used for power detection while the reflecting part is focused onto a CCD camera (DALSA CA-D1-0064A) which has 64×64 pixels and a grabbing rate of 2900 frames per second (fps). The SPGD algorithm built in a RT-Linux dual-core industrial computer is introduced to optimize the cost function (PIB). The control voltages for the DM are firstly generated from the computer with one 20-channel, 8-bit digital-to-analog (DA) converter, and then they are amplified by a high-voltage-amplifier (HVA) into $[-300\ \text{V}, 300\ \text{V}]$. At last, these voltages are applied onto the 19 actuators to drive the DM. On the basis of the SPGD algorithm, intracavity aberrations can be compensated in an iterative manner at an iterative rate of 2850 fps.

4 Experimental results of intracavity aberrations correction

We have accomplished a series of intracavity aberration correction experiments at different initial power levels. The ini-

tial output distributions depend on power, and more often than not, the higher the power, the more complex the initial output distributions. Figure 4 shows the relationship between the pumping power and the pumping current. Firstly, the pumping current is turned to 10.8 A, the output beam width is 4.3 mm, the output power is 3.6 W and the output laser mode looks like a TEM_{20} mode. After the AO system is switched on, the laser transverse intensity profile is Gaussian and the resulting output power increased to 3.9 W. Figure 5 shows the far-field beam distribution in the case of open loop and closed loop. What can be seen from Fig. 5 is that when the AO system is switched on, the laser spot becomes smaller, while the peak intensity on the CCD is improved from 135 to 250, which means that the energy on the CCD is centralized. This result may be explained as follows [13, 14]: in the course of PIB optimization, the DM changed its surface shape to counteract the intracavity aberrations (including thermal effects, spherical aberration and so on) continuously, and furthermore, since the DM is the rear mirror of the resonator, thus any change of the curvature radius of DM will result in a change in the resonator configuration, which may be capable of establishing conditions for generating the lower mode more efficiently while restraining the high-order transverse modes. During the course of the PIB optimization, the voltages on the DM actuators firstly vary quickly, and then converge to a group of values gradually. This real-time system can achieve an iterative calculation with a rate of 2850 fps while 500 to 700 frames are sufficient for an effective beam control based on this algorithm. From this point of view, the system has a control bandwidth of about 4 Hz. However, to control the mode keeping it as stable as possible, the distortions caused by ex-cavity environment in the lab should also be compensated, which will reduce the control bandwidth correspondingly. In the experiment we find that a stable and obvious enhancement of the far-field peak power at the pumping current of 10.8 A is obtained in less than 10 seconds.

When the pumping current is enhanced to 11.6 A, the output beam presents a TEM_{30}-like distribution with 5.1 W output, in this case, the output beam width is 5.2 mm, after several seconds, the mode is transformed into a Gaussian-like mode with 5.4 W output. The far-field intensity distributions at 11.6 A in both open loop and closed loop are shown in Fig. 6. The peak intensity on the CCD is increased from 105 to 225.

Similarly, Figs. 7 and 8 show far-field form distributions at the pumping current of 12 A, 12.3 A respectively. The output beam widths in two cases are 4.7 mm and 4.9 mm respectively, and after PIB optimization is finished, the TEM_{40}-like mode and a more complex mode are both transformed successfully into Gaussian-like modes. The output powers in the two cases are enhanced from 6.1 W, 7.2 W to 6.9 W and 7.6 W respectively, while the peak intensities of

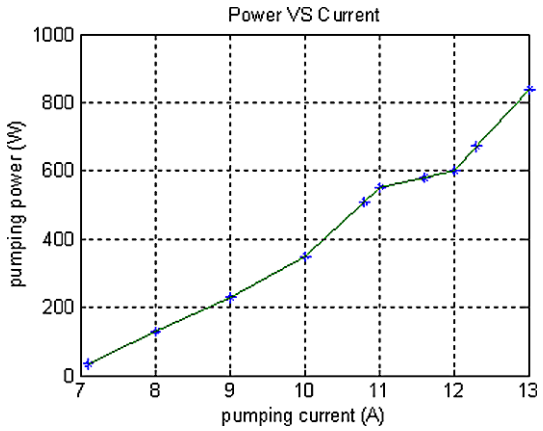

Fig. 4 Relationship of the pumping power and the pumping current

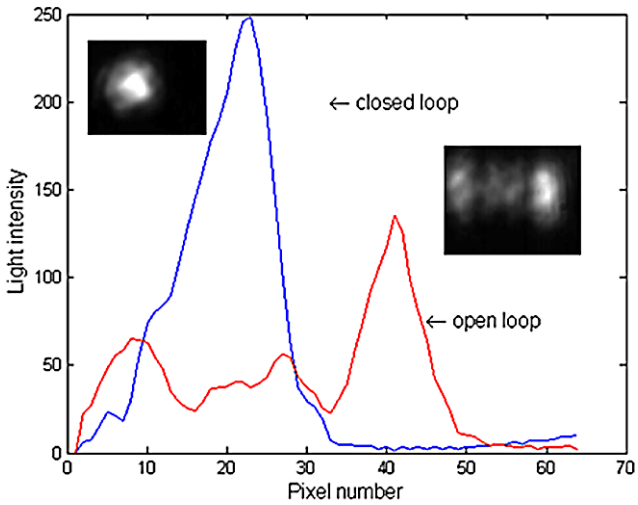

Fig. 5 The far-field laser form and intensity distributions in the case of open loop and closed loop at the pumping current of 10.8 A

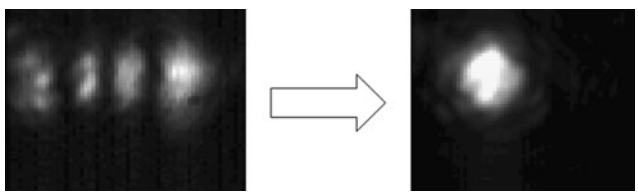

Fig. 6 The far-field laser form distributions in the case of open loop and closed loop at 11.6 A

two cases are increased from 95, 70 to 230 and 221 respectively.

Thanks to the high iterative rate, in all cases, the time cost for a stable aberrations correction can be restricted within 10 seconds, which guarantees the capability for correcting the slow dynamic thermal aberrations in the resonators. In all cases, when the AO system is off, the output beam intensity distribution and power are varying in some way while, when the AO system is switched on, they both become relative stable.

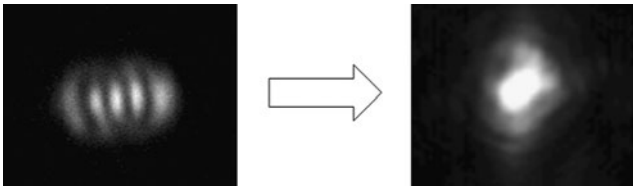

Fig. 7 The far-field laser form distributions in the case of open loop and closed loop at 12 A

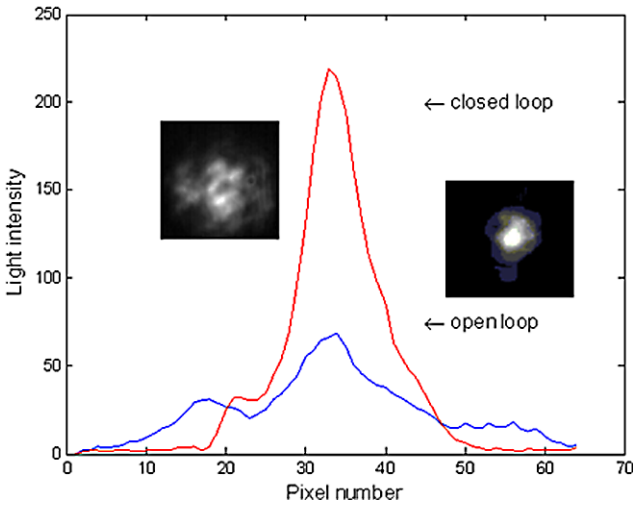

Fig. 8 The far-field laser intensity distributions in the case of open loop and closed loop at the pumping current of 12.3 A

Compared with the performance obtained in [13] and [14] (it costs at least one to several minutes to obtain an effective result), the most advantage of this system is speediness. The SPGD algorithm, in combination with the 2900 fps CCD and the RT-Linux dual-core industrial computer, can optimize the beam output nearly in real-time if the vapidly changing ex-cavity distortions are not considered to be corrected by our AO system. Besides, the results are more stable since the closed loop bandwidth is improved and is fast enough to compensate for the intracavity phase aberrations.

5 Conclusions

We have set up an adaptive intracavity aberrations correction system based on the SPGD control algorithm. The experimental results demonstrate that this system is capable of correcting the intracavity aberrations of a CW solid-state laser and enhancing its far-field peak power quickly and stably without added any pinhole in the resonator. Meanwhile, when the AO system is switched on, both the far-field peak power and intensity distributions become stable.

Acknowledgement This work was supported by the National Natural Science Foundation of China (Nos. 10974202 and 60978049) and the Chinese Academy of Sciences (Nos. A09K005 and CXJJ-10-S01).

References

1. A.A. Ishaaya, V. Eckhouse, L. Shimshi, N. Davidson, A.A. Friesem, Opt. Express **13**, 2722 (2005)
2. G. Machavariani, Appl. Opt. **43**, 6328 (2004)
3. H. Zimer, K. Albers, U. Wittrock, Opt. Lett. **29**, 2761 (2004)
4. U. Wittrock, I. Buske, H.M. Heuck, in *Conference on Lasers and Electro-Optics (CLEO)*, paper: CFM1 (2003)
5. P. Welp, H. .M. Heuck, U. Wittrock, in *European Conference on Lasers and Electro-Optics (CLEO_E)*, paper: CC_12 (2007)
6. P. Yang, S.J. Hu, X.D. Yang, S.Q. Chen, W. Yang, X. Zhang, B. Xu, SPIE Proc. **6108**, 182 (2005)
7. J.W. Hardy, *Adaptive Optics for Astronomical Telescope* (Oxford University Press, London, 1998)
8. W. Lubeigt, G. Valentine, J. Girkin, E. Bente, Opt. Express. **10**, 550 (2002)
9. D. Burns, G.J. Valentine, W. Lubeigt, E. Bente, A.I. Ferguson, Proc. SPIE **4629**, 4629 (2002)
10. W. Lubeigt, G.J. Valentine, Opt. Express. **16**, 10943 (2008)
11. A.A. Aleksandrov, A.V. Kudryashov, A.L. Rukosuev, T.Yu. Cherezova, Yu.V. Sheldakova, J. Opt. Technol. **74**, 550 (2007)
12. Tatyana Yu. Cherezova, Leonid N. Kaptsov, Alexis V. Kudryashov, Appl. Opt. **35**, 2554 (1996)
13. P. Yang, M.W. Ao, Y. Liu, B. Xu, W.H. Jiang, Opt. Express. **15**, 17051 (2007)
14. P. Yang, Y. Liu, W. Yang, M.W. Ao, S.J. Hu, B. Xu, W.H. Jiang, Opt. Commun. **278**, 377 (2007)
15. W.H. Jiang, N. Ling, X.B. Wu, C.H. Wang, H. Xian, S.F. Jiang, Z.J. Rong, C.L. Guan, L.T. Jiang, Z.B. Gong, Y. Wu, Y.J. Wang, Proc. SPIE **2828**, 312 (1996)
16. M.A. Vorontsov, G.W. Carhart, J.C. Ricklin, Opt. Lett. **22**, 907 (1997)